

# Effect of Three-Body Interactions between Dissimilar Molecules on the Phase Behavior of Binary Mixtures: The Transition from Vapor–Liquid Equilibria to Type III Behavior<sup>†</sup>

Richard J. Sadus\*

Computer Simulation and Physical Applications Group, School of Information Technology, Swinburne University of Technology, P.O. Box 218, Hawthorn, Victoria 3122, Australia

An investigation is reported of the effect of three-body interactions between dissimilar molecules on the phase behavior of binary mixtures. The Gibbs ensemble algorithm is implemented to determine phase coexistence of binary mixtures interacting via a two-body Lennard–Jones + three-body Axilrod–Teller potential. The contributions of both two-body and three-body interactions are calculated exactly. Calculations are reported with three-body interactions of varying strength. It is demonstrated that three-body interactions can result in a transition from vapor–liquid equilibria to type IIIb behavior (gas–gas immiscibility of the second kind). This is the first time that three-body interactions have been linked rigorously to type III behavior.

## 1. Introduction

Knowledge of intermolecular interactions is important for the theoretically based prediction of the phase behavior of fluids and fluid mixtures. It is well documented (Sadus, 1992) that the phase behavior of binary mixtures changes in accordance with a variation in the strength of interaction between pairs of dissimilar molecules. In terms of the classification scheme of van Konynenburg and Scott (1980), strong pair interaction is associated with type I behavior in which only vapor–liquid coexistence is possible. If the dissimilar pair interaction is weak, liquid–liquid equilibria is observed, which is most commonly associated with either type II or type III behavior. It has been assumed almost universally that the phase behavior of fluids can be attributed exclusively to interaction between pairs of molecules, and calculations (Sadus, 1992) routinely ignore the contributions of three- or more-body interactions. However, the available evidence (Barker et al., 1971; Monson et al., 1983; Rittger, 1990a–c; Elrod and Saykally, 1994) suggests that the effect of three-body interactions may be important in some circumstances. For example, it is reported typically (Barker et al., 1972a) that a two-body plus an Axilrod–Teller potential (Axilrod and Teller, 1943) improves the prediction of third virial coefficients of atomic systems. Three-body interactions also appear to have a greater role in molecular fluids (Monson et al., 1983; Elrod and Saykally, 1994). Nevertheless, the exact role of three-body interactions remains unclear partly because attempts to account for three-body interactions commonly involve approximations.

In principle, molecular simulation (Allen and Tildesley, 1987) can be used to calculate three-body interactions rigorously. However, the use of molecular simulation has been restricted largely to pairwise interactions and, until recently the few studies (Barker et al., 1971; Monson et al., 1983; Smit et al., 1992; Miyano, 1995;

Sadus and Prausnitz, 1996; Sadus, 1996) that have attempted to include three-body interactions have relied on various approximations rather than rigorous calculation. Recently, Anta et al. (1997) and Sadus (1997a) reported exact calculations of the effect of three-body interactions on the vapor–liquid equilibria of pure fluids. The results of these independent studies indicate that Axilrod–Teller interactions can significantly alter the density of the liquid branch of the coexistence curve. Sadus (1997b) also reported that three-body interactions can have a profound effect on the liquid–liquid equilibria of binary mixtures.

This work examines the effect of three-body interactions between dissimilar molecules on the vapor–liquid behavior of binary mixtures. The Gibbs ensemble (Panagiotopoulos et al., 1988) is used to calculate the liquid–liquid-phase coexistence of binary mixtures, with components interacting via a Lennard–Jones + Axilrod–Teller intermolecular potential. The calculation of three-body interactions is exact, with both two- and three-body interactions contributing to the acceptance criterion of each attempted Monte Carlo move.

## 2. Theory

**2.1. Intermolecular Potential.** The intermolecular potential ( $u$ ) is the sum of contributions from two-body interactions ( $u(ij)$ ) and three-body dispersion interactions ( $u(ijk)$ ):

$$u = u(ij) + u^{\text{disp}}(ijk) \quad (1)$$

The Lennard–Jones potential was used to calculate interactions between pairs of molecules separated by a distance  $r_{ij}$ :

$$u(ij) = 4\epsilon \left[ \left( \frac{\sigma}{r_{ij}} \right)^{12} - \left( \frac{\sigma}{r_{ij}} \right)^6 \right] \quad (2)$$

where the  $\epsilon$  and  $\sigma$  parameters are characteristic of the strength of intermolecular interaction and molecular size, respectively.

The Axilrod–Teller term (Axilrod and Teller, 1943) accounts for the contribution of three-body dispersion

\* Author to whom correspondence should be sent. E-mail: RSadus@swin.edu.au.

<sup>†</sup> Dedicated to Professor John M. Prausnitz on the occasion of his 70th birthday.

interactions:

$$u^{\text{disp}}(ijk) = \frac{\nu(1 + 3 \cos \theta_i \cos \theta_j \cos \theta_k)}{(r_{ij}r_{ik}r_{jk})^3} \quad (3)$$

where  $\theta$  refers to the inside angles of a triangle formed by three molecules  $i$ ,  $j$ , and  $k$ , and  $\nu$  is the nonadditive coefficient. This potential is negative for near-linear configurations and positive for acute triangular arrangements.

**2.2. Potential Parameters.** The calculations were performed in reduced units relative to component 1. The parameters for the Lennard–Jones potentials were  $\epsilon_{22}/\epsilon_{11} = 0.5$ ,  $\sigma_{22}/\sigma_{11} = 1$ ,  $\epsilon_{12} = \sqrt{\epsilon_{11}\epsilon_{22}}$  and  $\sigma_{12} = (\sigma_{11} + \sigma_{22})/2$ . This combination of parameters was chosen because earlier work (Sadus, 1996) on Lennard–Jones mixtures indicated that they are associated with a closed vapor–liquid-phase envelope.

For the Axilrod–Teller potential, we must consider the nonadditive coefficient arising from triplets composed of different combinations of the component molecules. There are four distinct possible combinations of three molecules in a binary mixture. The nonadditive coefficient of component 2 molecules was related to component 1 by:

$$\nu_{222} = \alpha\nu_{111} \quad (4)$$

where  $\alpha$  is an arbitrary adjustable parameter. A value of  $\nu_{111}/\epsilon_{11}\sigma_{11}^9 = 0.0712$  was used which corresponds to the nonadditive coefficient of an atom such as argon (Leonard and Barker, 1975). The unlike nonadditive coefficients were obtained by taking a geometric average of the like interactions.

$$\nu_{112} = \sqrt[3]{\nu_{111}\nu_{111}\nu_{222}} \quad (5)$$

$$\nu_{122} = \sqrt[3]{\nu_{111}\nu_{222}\nu_{222}} \quad (6)$$

Comparison of the results of these combining rules with experimental nonadditive coefficients for the noble gases (Leonard and Barker, 1975) indicate that they are accurate.

**2.3. Simulation Details.** The NPT–Gibbs ensemble (Panagiotopoulos et al., 1988) was used to simulate the coexistence of two phases. A total of 200 molecules were partitioned between two boxes to simulate the two coexisting phases. The temperature of the entire system was held constant and surface effects were avoided by placing each box at the center of a periodic array of identical boxes. Equilibrium was achieved by attempting molecular displacements (for internal equilibrium), volume fluctuations (for mechanical equilibrium), and particle interchanges between the boxes (for material equilibrium).

The simulations were performed in cycles with each cycle consisting of 200 attempted displacements, a single volume fluctuation, and 500 interchange attempts. The maximum molecular displacement and volume changes were adjusted to obtain, where possible, a 50% acceptance rate for the attempted move. Ensemble averages were accumulated only after the system had reached equilibrium. The equilibration period was typically 2500 cycles and a further 2500 cycles were used to accumulate the averages. The calculations were truncated at intermolecular separations greater than

half the box length, and appropriate long-range corrections (Allen and Tildesley, 1987) were used to obtain the full contribution of pair interactions to energy and pressure. The full (untruncated) three-body potential was calculated to avoid uncertainties that arise when calculating three-body, long-range corrections from unknown pair-distribution functions. Alternative computational approaches for long-range corrections are available (Rittger, 1992).

The contributions of both two- and three-body interactions to the configurational energy of the fluid were recalculated for each attempted move, and the configurational properties were updated after each successful move. Therefore, changes to both two- and three-body interactions contributed to the acceptance criterion and the predicted phase coexistence curve is the result of two- and three-body interactions. A typical run required ~57 CPU hours on a Cray YMP-EL and 9 CPU hours on a Fujitsu VPP300 supercomputer.

### 3. Results

The phase coexistence data obtained from molecular simulation at  $T^* = 0.9$  are summarized in Tables 1–3. The normal convention was adopted for the reduced density ( $\rho^* = \rho\sigma^3$ ), temperature ( $T^* = kT/\epsilon$ ), energy ( $E^* = E/\epsilon$ ), pressure ( $P^* = P\sigma^3$ ), and chemical potential ( $\mu^* = \mu/\epsilon$ ). The chemical potential was determined from the equation proposed by Smit and Frenkel (1989). In Tables 1–3 the contribution of Lennard–Jones (LJ) and Axilrod–Teller (AT) interactions to both the energy and pressure are identified.

### 4. Discussion

Simulations were performed at different relative strengths of three-body interactions between the components of the mixture governed by the parameter  $\alpha$ . A value of  $\alpha = 0$  indicates that three-body interaction is restricted exclusively to triplets of component 1;  $\alpha = 0.5$  indicates that three-body interaction of component 2 molecules is half as strong as component 1 molecules; and  $\alpha = 1$  indicates identically strong three-body interaction for both components. A temperature of  $T^* = 0.9$  was used for all simulations because previous simulation results (Sadus, 1996) demonstrate that the Lennard–Jones fluid exhibits a substantial vapor–liquid-phase envelope at this temperature.

Simulation results for  $\alpha = 0$  are summarized in Table 1 and the pressure–composition behavior is compared with that of a Lennard–Jones fluid in Figure 1. Figure 1 shows that both systems have a closed vapor–liquid envelope. The effect of three-body interactions is to substantially lower the critical point of the mixture. A similar effect has been observed (Anta et al., 1997; Sadus, 1997a) for the critical point of pure fluids. It should be noted that the Gibbs ensemble cannot be used to accurately approach the critical point, and other techniques such as finite-size scaling (Wilding, 1997) are more useful in the near critical region. A value of  $\alpha = 0$  implies that three-body interactions are confined exclusively to component 1. The relatively small contribution of Axilrod–Teller interactions to both the energy and pressure reported in Table 1 reflects the small probability finding triplets exclusively of component 1. In real mixtures, there will also be three-body interactions between molecules of component 2 and with triplets containing both components. However, if three-

**Table 1. Gibbs-Ensemble Simulation of Phase Equilibria at  $T^* = 0.9$  Using the Lennard-Jones + Axilrod-Teller Intermolecular Potential with  $\alpha = 0^a$** 

Phase A								
$P^*$	$\rho^*$	$x_1$	$-E_{LJ}^*$	$E_{AT}^*$	$-P_{LJ}^*$	$P_{AT}^*$	$-\mu_1^*$	$-\mu_2^*$
0.072	0.671(27)	0.797(63)	4.02(27)	0.10(3)	0.77(10)	0.21(7)	3.92	2.88
0.075	0.678(21)	0.789(53)	4.01(30)	0.10(3)	0.75(7)	0.21(6)	3.85	2.77
0.085	0.672(8)	0.755(27)	3.85(13)	0.09(1)	0.70(5)	0.17(3)	3.87	2.73
0.088	0.670(27)	0.723(80)	3.78(40)	0.08(3)	0.69(8)	0.17(7)	3.84	2.76
0.089	0.626(19)	0.574(65)	3.18(22)	0.04(1)	0.57(5)	0.07(3)	3.75	2.76
Phase B								
$P^*$	$\rho^*$	$x_1$	$-E_{LJ}^*$	$E_{AT}^*$	$-P_{LJ}^*$	$P_{AT}^*$	$-\mu_1^*$	$-\mu_2^*$
0.072	0.095(4)	0.231(14)	0.50(3)	0.00011(6)	0.023(2)	0.00003(2)	3.97	2.85
0.075	0.120(9)	0.225(24)	0.62(10)	0.00022(9)	0.037(7)	0.00005(2)	3.91	2.76
0.085	0.130(9)	0.221(20)	0.66(6)	0.00018(9)	0.043(6)	0.00007(4)	3.90	2.72
0.088	0.158(17)	0.231(24)	0.79(9)	0.00027(9)	0.060(10)	0.00014(6)	3.84	2.69
0.089	0.251(142)	0.277(93)	1.12(70)	0.005(10)	0.16(15)	0.008(18)	3.82	2.72

<sup>a</sup> Values in parentheses indicate the uncertainty in the last digit.

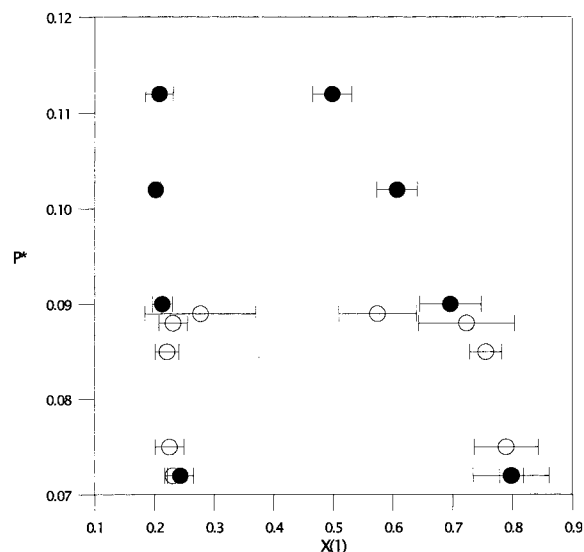


**Figure 1.** Comparison of the pressure-composition projection of the vapor-liquid equilibria of a binary Lennard-Jones (●, Sadus, 1996) and a Lennard-Jones + Axilrod-Teller (○,  $\alpha = 0$ ) mixture.

body interaction is confined to only one component, Figure 1 indicates that the effect is primarily to restrict vapor-liquid equilibria to lower pressures.

Simulations with  $\alpha = 0.5$  reflect three-body interactions in a binary mixture more realistically. The results are summarized in Table 2 and the pressure-composition behavior is illustrated in Figure 2. In contrast to either the Lennard-Jones fluid or the case when  $\alpha = 0$ , a closed vapor-liquid envelope is not observed. In the vicinity of  $P^* = 0.1$ , the vapor-liquid envelope approaches closure but instead, the vapor branch is transformed into a second liquid branch and liquid-liquid equilibria is observed at higher pressures. The transition between vapor-liquid and liquid-liquid equilibria is illustrated clearly on the pressure-density projection in Figure 3. The liquid branch of the coexistence curve is characterized by two distinct parts above and below a density minimum in the vicinity of  $P^* = 0.1$ . In contrast, the density of the vapor branch increases progressively with increasing pressure until it attains liquidlike densities. There is a continuous transition between vaporlike and liquidlike phenomena.

The phenomenon exhibited in Figures 2 and 3 is characteristic of type III equilibria in accordance with the classification scheme of van Konynenburg and Scott

(1980), who classified the phase behavior of binary mixtures into five or six basic types depending on the nature of critical equilibria. The majority of commonly occurring binary mixtures can be classified as either type I, II, or III (Sadus, 1992). The simplest critical behavior is exhibited by a type I mixture, which consists of a continuous locus of vapor-liquid critical points linking the critical points of the pure components. The critical properties of type II mixtures are characterized by separate regions of vapor-liquid and liquid-liquid equilibria. In addition to a continuous critical line between the components, type II mixtures exhibit a locus of upper critical solution temperatures (UCST) commencing at an upper critical end point (UCEP) on the end of a three-phase liquid-liquid-vapor line. The UCEP is normally found at a temperature well below the critical temperature of either component and the locus of UCSTs rises steeply to very high pressures. In contrast, type III behavior is characterized by a discontinuity of vapor-liquid equilibria. Commencing from the critical point of the component with the lowest critical temperature, a locus of vapor-liquid equilibria typically extends partly toward the critical temperature of the other component before being terminated by an UCEP at the end of a three-phase liquid-liquid-vapor line. A second critical line commences from the critical point of the component with the highest critical temperature rising to very high pressures and never meeting the critical point of the other component. A continuous transition from vapor-liquid to liquid-liquid equilibria is observed along this higher temperature critical line. Two distinct categories of type III equilibria are possible depending on the behavior of the higher temperature critical line. In type IIIa behavior, a critical line starts from the vapor-liquid critical point of the component with the highest critical temperature and extends to still higher temperatures. This phenomenon is sometimes referred to as "gas-gas immiscibility of the first kind" and it is observed typically for binary mixtures containing helium (Stretenskaja et al., 1995; Wei and Sadus, 1996). Alternatively, in type IIIb mixtures, the critical line extends initially to lower temperatures before passing through a temperature minimum and subsequently attaining temperatures above the critical temperature of either pure component. This phenomenon is sometimes referred to as "gas-gas immiscibility of the second kind" (Shmonov et al., 1993). The pressure-composition behavior illustrated in Figure 2 is characteristic of the pressure-composition

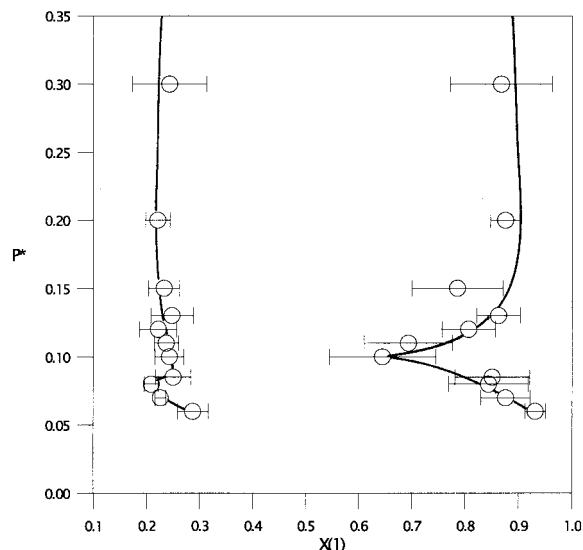
**Table 2. Gibbs-Ensemble Simulation of Phase Equilibria at  $T^* = 0.9$  Using the Lennard-Jones + Axilrod-Teller Intermolecular Potential with  $\alpha = 0.5^a$** 

Phase A								
$P^*$	$\rho^*$	$x_1$	$-E_{LJ}^*$	$E_{AT}^*$	$-P_{LJ}^*$	$P_{AT}^*$	$-\mu_1^*$	$-\mu_2^*$
0.06	0.698(18)	0.931(19)	4.67(20)	0.20(2)	0.91(8)	0.42(4)	3.67	2.96
0.07	0.686(18)	0.876(46)	4.39(28)	0.18(2)	0.88(4)	0.37(5)	3.71	2.76
0.08	0.674(34)	0.844(74)	4.21(44)	0.17(3)	0.84(9)	0.35(7)	3.83	2.75
0.10	0.588(57)	0.645(100)	3.19(55)	0.11(3)	0.63(11)	0.19(8)	3.79	2.70
0.11	0.622(28)	0.694(83)	3.45(36)	0.12(2)	0.69(10)	0.23(5)	3.78	2.67
0.12	0.675(18)	0.807(50)	4.08(27)	0.16(2)	0.83(8)	0.33(4)	3.73	2.57
0.15	0.661(25)	0.786(85)	3.93(40)	0.15(3)	0.79(11)	0.30(6)	3.73	2.60
0.20	0.702(13)	0.876(28)	4.47(19)	0.19(1)	0.83(6)	0.40(4)	3.58	2.51
0.30	0.722(19)	0.868(95)	4.59(45)	0.20(3)	0.78(10)	0.44(7)	3.38	2.41

Phase B								
$P^*$	$\rho^*$	$x_1$	$-E_{LJ}^*$	$E_{AT}^*$	$-P_{LJ}^*$	$P_{AT}^*$	$-\mu_1^*$	$-\mu_2^*$
0.06	0.079(7)	0.287(29)	0.42(4)	0.0021(4)	0.017(4)	0.0005(1)	3.88	2.99
0.07	0.122(8)	0.226(10)	0.63(5)	0.0049(8)	0.038(6)	0.0018(4)	3.88	2.74
0.08	0.106(6)	0.209(13)	0.53(2)	0.0035(4)	0.028(3)	0.0011(2)	3.79	2.77
0.10	0.141(22)	0.243(27)	0.69(10)	0.007(2)	0.05(2)	0.003(2)	3.82	2.72
0.11	0.226(111)	0.237(23)	1.06(47)	0.017(14)	0.13(11)	0.017(21)	3.83	2.68
0.12	0.297(50)	0.222(35)	1.39(23)	0.023(7)	0.18(5)	0.0217(9)	3.83	2.60
0.15	0.410(41)	0.233(29)	1.85(17)	0.041(8)	0.31(6)	0.05(2)	3.81	2.63
0.20	0.579(33)	0.221(23)	2.53(16)	0.073(9)	0.48(3)	0.13(2)	3.67	2.50
0.30	0.635(26)	0.243(70)	2.78(15)	0.089(9)	0.48(5)	0.17(2)	3.52	2.37

<sup>a</sup> Values in parentheses indicate the uncertainty in the last digit.



**Figure 2.** Pressure-composition projection at  $T^* = 0.9$  of the phase behavior of a Lennard-Jones + Axilrod-Teller binary mixture with  $\alpha = 0.5$ .

projection of type IIIb mixtures at temperatures less than the critical temperature minimum. Therefore, liquid-liquid equilibria for this system will persist to very high pressures without reaching a critical point.

When the strength of three-body interactions of both components is equal ( $\alpha = 1$ ), the phase behavior of the mixture is also characteristic of type IIIb phenomena (Figures 4 and 5). The "transitional" behavior between vapor-liquid and liquid-liquid equilibria occurs at pressures in the vicinity of  $P^* = 0.25$ .

It is interesting to note that the transition between vapor-liquid and type IIIb behavior occurs despite the fact that the contribution of three-body interactions to the configurational energy of the fluid is relatively small. The value of  $|E_{AT}^*|$  reported in Tables 3 and 4 is typically only between 2 and 4% of  $|E_{LJ}^*|$ . In contrast, the contribution of three-body interactions to the pressure is significant. The value of  $|P_{AT}^*|$  reported in Tables 3 and 4 can be as high as 60% of  $|P_{LJ}^*|$ . It is

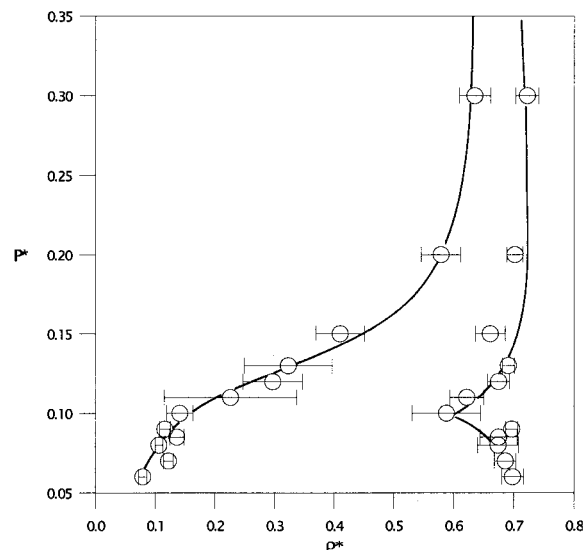


**Figure 3.** Pressure-density projection at  $T^* = 0.9$  of the phase behavior of a Lennard-Jones + Axilrod-Teller binary mixture with  $\alpha = 0.5$ .

apparent that the transition between vapor-liquid and type IIIb is very sensitive to three-body interactions.

It should be noted that the combination of the Lennard-Jones and Axilrod-Teller potentials represents a model description of intermolecular interactions. Consequently, any conclusions made from these simulation results for real mixtures must be tempered by the limitations of the intermolecular potentials used. Even for the noble gases, more sophisticated potentials (Barker et al., 1974; Aziz and Slaman, 1986) are required to account very accurately for two-body interactions. Recently, Anta et al. (1997) showed that the combination of the Aziz-Slaman potential (Aziz and Slaman, 1986) and the Axilrod-Teller term improves the accuracy of the calculated vapor-liquid equilibria of pure argon. The Axilrod-Teller potential only represents the contribution of dipoles to three-body interactions. Other higher multipole terms can also contribute to three-body interactions but their effect is generally both negligible

**Table 3. Gibbs-Ensemble Simulation of Liquid-Liquid Equilibria at  $T^* = 0.9$  Using the Lennard-Jones + Axilrod-Teller Intermolecular Potential with  $\alpha = 1.0^a$** 

Phase A								
$P^*$	$\rho^*$	$x_1$	$-E_{LJ}^*$	$E_{AT}^*$	$-P_{LJ}^*$	$P_{AT}^*$	$-\mu_1^*$	$-\mu_2^*$
0.05	0.706(19)	0.950(16)	4.81(20)	0.21(1)	0.94(7)	0.45(4)	3.72	2.89
0.08	0.679(13)	0.892(24)	4.38(18)	0.19(1)	0.90(7)	0.39(3)	3.82	2.73
0.10	0.678(18)	0.865(47)	4.28(29)	0.19(2)	0.86(6)	0.38(4)	3.76	2.67
0.15	0.679(23)	0.835(60)	4.19(32)	0.18(2)	0.82(6)	0.38(5)	3.78	2.54
0.20	0.700(21)	0.868(47)	4.43(33)	0.20(2)	0.84(7)	0.42(6)	3.58	2.47
0.25	0.715(24)	0.900(48)	4.66(34)	0.22(2)	0.80(7)	0.47(6)	3.48	2.43
0.27	0.723(10)	0.927(26)	4.83(16)	0.22(8)	0.87(12)	0.49(2)	3.48	2.44
0.30	0.705(16)	0.881(31)	4.50(20)	0.20(1)	0.82(5)	0.44(4)	3.48	2.41
0.40	0.731(10)	0.895(42)	4.73(23)	0.22(1)	0.74(5)	0.49(3)	3.29	2.17
Phase B								
$P^*$	$\rho^*$	$x_1$	$-E_{LJ}^*$	$E_{AT}^*$	$-P_{LJ}^*$	$P_{AT}^*$	$-\mu_1^*$	$-\mu_2^*$
0.05	0.075(3)	0.301(31)	0.39(2)	0.0029(3)	0.015(2)	0.00065(9)	3.72	2.89
0.08	0.116(10)	0.224(14)	0.59(5)	0.007(2)	0.036(5)	0.0026(7)	3.90	2.75
0.10	0.171(26)	0.218(28)	0.84(12)	0.015(4)	0.08(2)	0.008(3)	3.83	2.63
0.15	0.303(21)	0.202(21)	1.40(11)	0.040(6)	0.19(3)	0.037(9)	3.82	2.54
0.20	0.481(50)	0.254(50)	2.13(20)	0.09(2)	0.41(6)	0.13(3)	3.70	2.51
0.25	0.551(40)	0.329(29)	2.46(19)	0.10(2)	0.47(5)	0.17(3)	3.55	2.44
0.27	0.554(34)	0.304(18)	2.46(13)	0.11(1)	0.46(5)	0.18(4)	3.57	2.42
0.30	0.575(35)	0.223(54)	2.50(12)	0.12(2)	0.48(4)	0.22(4)	3.57	2.35
0.40	0.622(24)	0.204(39)	2.69(10)	0.15(2)	0.50(3)	0.28(4)	3.44	2.17

<sup>a</sup> Values in parentheses indicate the uncertainty in the last digit.

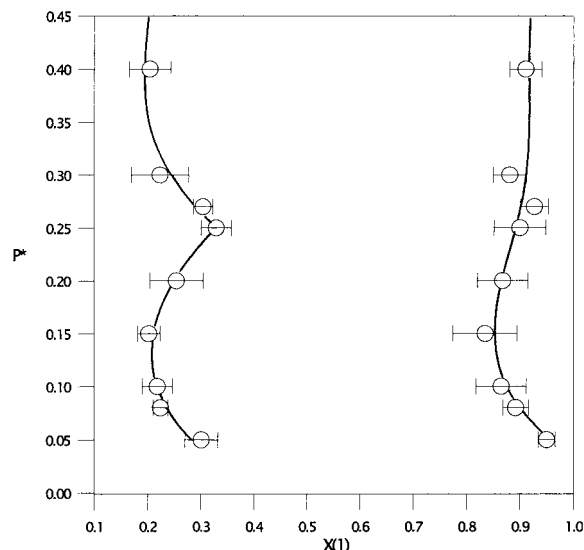


**Figure 4.** Pressure-composition projection at  $T^* = 0.9$  of the phase behavior of a Lennard-Jones + Axilrod-Teller binary mixture with  $\alpha = 1$ .

(Elrod and Saykally, 1994; Rittger, 1990) and offset by a fourth-order, triple-dipole term (Barker et al., 1972b). More importantly, the effect of Axilrod-Teller interactions may be offset substantially (Elrod and Saykally, 1994; Sadus and Prausnitz, 1996) by repulsive interactions from three-body overlap.

## 5. Conclusions

For the first time, it is demonstrated that three-body interactions can induce a transition from vapor-liquid equilibria to type IIIb behavior in a model fluid. The transition is observed despite the fact that three-body interactions make a relatively small contribution to the overall energy of the fluid. However, any inference for real fluids must be tempered by the limitations of the intermolecular potentials used. In particular, in real fluids the effect of three-body overlap may offset partially the influence of the Axilrod-Teller potential.

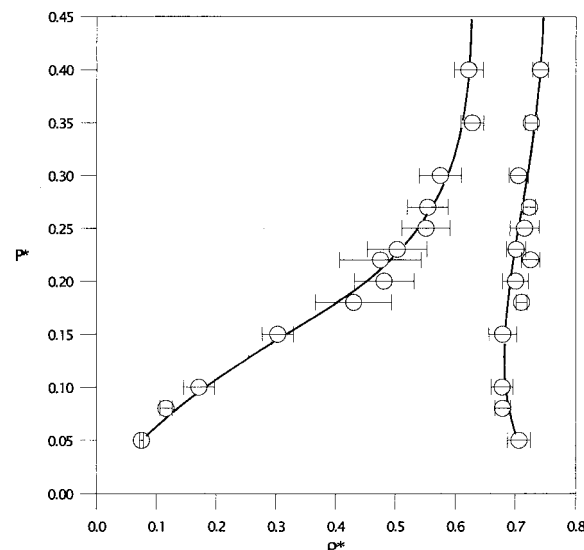


**Figure 5.** Pressure-density projection at  $T^* = 0.9$  of the phase behavior of a Lennard-Jones + Axilrod-Teller binary mixture with  $\alpha = 1$ .

## Acknowledgment

The simulations were performed on the Swinburne University of Technology's Cray YMP-EL computer and the Australian National University Supercomputer Centre's Fujitsu VPP300 supercomputer.

## Nomenclature

- $A$  = phase identifier
- $B$  = phase identifier
- $E$  = configurational energy
- $k$  = Boltzmann's constant
- $P$  = pressure
- $r$  = intermolecular distance
- $T$  = temperature
- UCEP = upper critical end point
- UCST = upper critical solution temperature
- $u$  = intermolecular potential
- $x_1$  = mole fraction of component 1

*Greek Alphabet*

- $\alpha$  = adjustable parameter  
 $\epsilon$  = Lennard–Jones energy parameter  
 $\sigma$  = Lennard–Jones distance parameter  
 $\rho$  = number density  
 $\theta$  = intramolecular angle  
 $\nu$  = nonadditive coefficient

*Subscripts and Superscripts*

- \* = reduced property  
 AT = Axilrod–Teller  
 disp = dispersion  
 $i, j, k$  = molecule  $i, j$ , or  $k$   
 LJ = Lennard–Jones

**Literature Cited**

- Allen, M. P.; Tildesley, D. J. *Computer Simulation of Liquids*; Clarendon: Oxford, 1987.
- Anta, J. A.; Lomba, E.; Lombardero, M. Influence of Three-Body Forces on the Gas–Liquid Coexistence of Simple Fluids: The Phase Equilibrium of Argon. *Phys. Rev. E* **1997**, *55*, 2707.
- Axilrod, B. M.; Teller, E. Interaction of the van der Waals' Type Between Three Atoms. *J. Chem. Phys.* **1943**, *11*, 299.
- Aziz, R. A.; Slaman, M. J. The Argon and Krypton Interatomic Potentials Revisited. *Mol. Phys.* **1986**, *58*, 679.
- Barker, J. A.; Fisher, R. A.; Watts, R. O. Liquid Argon: Monte Carlo and Molecular Dynamics Calculations. *Mol. Phys.* **1971**, *21*, 657.
- Barker, J. A.; Johnson, C. H. J.; Spurling, T. H. Third Virial Coefficients for Krypton. *Aust. J. Chem.* **1972a**, *25*, 1813.
- Barker, J. A.; Johnson, C. H. J.; Spurling, T. H. On the Cancellation of Certain Three- and Four-Body Interactions in Inert Gases. *Aust. J. Chem.* **1972b**, *25*, 1811.
- Barker, J. A.; Watts, R. O.; Lee, J. K.; Schafer, T. P.; Lee, Y. T. Interatomic Potentials for Krypton and Xenon. *J. Chem. Phys.* **1974**, *61*, 3081.
- Elrod, M. J.; Saykally, R. J. Many-Body Effects in Intermolecular Forces. *Chem. Rev.* **1994**, *94*, 1975.
- Leonard, P. J.; Barker, J. A. In *Theoretical Chemistry: Advances and Perspectives*, Vol. 1; Eyring, H., Henderson, D., Eds.; Academic: London, 1975.
- Miyano, Y. An Effective Triplet Potential for Argon. *Fluid Phase Equilib.* **1994**, *95*, 31.
- Monson, A. P.; Rigby, M.; Steele, W. A. Non-Additive Energy Effects in Molecular Liquids. *Mol. Phys.* **1983**, *49*, 893.
- Panagiotopoulos, A. Z.; Quirke, N.; Stapleton, M.; Tildesley, D. J. Phase Equilibria by Simulation in the Gibbs Ensemble: Alternative Derivation, Generalization and Application to Mixture and Membrane Equilibria. *Mol. Phys.* **1988**, *63*, 527.
- Rittger, E. The Chemical Potential of Liquid Xenon by Computer Simulation. *Mol. Phys.* **1990a**, *69*, 853.
- Rittger, E. Can Three-Atom Potentials be Determined from Thermodynamic Data? *Mol. Phys.* **1990b**, *69*, 867.
- Rittger, E. An Empirical Three-atom Potential for Xenon. *Mol. Phys.* **1990c**, *71*, 79.
- Rittger, E. Handling Three-Body Potentials in Computer Simulation. *Comput. Phys. Commun.* **1992**, *67*, 412.
- Sadus, R. J. *High-Pressure Phase Behaviour of Multicomponent Fluid Mixtures*; Elsevier: Amsterdam, 1992.
- Sadus, R. J. Monte Carlo Simulation of Vapour–Liquid Equilibria in “Lennard–Jones + Three-Body Potential” Binary Fluid Mixtures. *Fluid Phase Equilib.* **1996**, *116*, 289.
- Sadus, R. J. Exact Calculation of the Effect of Three-Body Axilrod–Teller Interactions on Vapour–Liquid–Phase Coexistence. *Fluid Phase Equilib.* **1997a**, in press.
- Sadus, R. J. The Effect of Three-Body Interactions on the Liquid–Liquid Equilibria of Binary Fluid Mixtures. *Fluid Phase Equilib.* **1997b**, in press.
- Sadus, R. J.; Prausnitz, J. M. Three-Body Interactions in Fluids from Molecular Simulation: Vapor–Liquid–Phase Coexistence of Argon. *J. Chem. Phys.* **1996**, *104*, 4784.
- Shmonov, V. M.; Sadus, R. J.; Franck, E. U. High-Pressure Phase Equilibria and Supercritical pVT Data of the Binary Water + Methane Mixture to 723 K and 200 MPa. *J. Phys. Chem.* **1993**, *97*, 9054.
- Smit, B.; Frenkel, D. Calculation of the Chemical Potential in the Gibbs Ensemble. *Mol. Phys.* **1989**, *68*, 951.
- Smit, B.; Hauschild, T.; Prausnitz, J. M. Effect of a Density-Dependent Potential on the Phase Behaviour of Fluids. *Mol. Phys.* **1992**, *77*, 1021.
- Stretenskaja, N. G.; Sadus, R. J.; Franck, E. U. High-Pressure Phase Equilibria and Critical Curve of the Water + Helium System to 200 MPa and 723 K. *J. Phys. Chem.* **1995**, *99*, 4273.
- Van Konynenburg, P. H.; Scott, R. L. Critical Lines and Phase Equilibria in Binary van der Waals Mixtures. *Philos. Trans. R. Soc. London A* **1980**, *298*, 495.
- Wei, Y. S.; Sadus, R. J. Vapour–Liquid–Phase Equilibria of Binary Mixtures Containing Helium: Comparison of Experiment with Predictions Using Equations of State. *Fluid Phase Equilib.* **1996**, *11*, 1.
- Wilding, N. B. Simulation Studies of Fluid Critical Behaviour. *J. Phys.: Condens. Matter* **1997**, *9*, 585.

Received for review November 20, 1997

Revised manuscript received January 23, 1998

Accepted January 23, 1998

IE970809T